Journal of Mathematical Extension
Vol. 20, No. 2 (2026) (1) 1-30
ISSN: 1735-8299
URL: http://doi.org/10.30495/JME.2026.3289
Original Research Paper

The Novel Dynamic Interrupted Autoregressive Model Based on the Split Normal Innovations

F. Pooyannik
Islamic Azad University, Marvdasht Branc

Z. Khodadadi*
Islamic Azad University, Marvdasht Branc

Abstract. The main purpose of the paper is to introduce a new interrupted model, whereas the asymmetric nature of real data is well considered in modeling. Also, the autoregressive coefficient of the model before and after intervention may be changed, which is covered in the proposed model. The transfer function of the proposed process is designed to follow a dynamic step change structure. The Bayesian estimation of the unknown parameters of the model is provided, as well as the prior and posterior distributions of the parameters. By considering Markov chain Monte Carlo samples, the convergence of the proposed estimation approach is verified. Real data on new weekly COVID-19 cases from Greece, from March 1, 2020, to December 17, 2023, confirms the applicability of the proposed model.

AMS Subject Classification: 62M10.
Keywords and Phrases: Bayesian Estimation, Interrupted Autoregressive, Innovations, Split Normal Distribution

Received: February 2025 ; Accepted: December 2025
*Corresponding Author

1 Introduction

In some real situations, a major exterior event or exposure known as an intervention causes a process to change significantly, providing an opportunity to better understand the dynamics and characteristics of that process. These intentional or unintentional actions can offer unique insights into environmental, social, or physical phenomena that would otherwise be inaccessible. Typically, this involves using intervention time series (ITS) analysis, which examines how unexpected events influence time series data by the collection of sequential data at multiple stages during which interventions are applied to assess the intervention's impact on outcomes. ITS employs quasi-experimental modeling techniques that depend on assumptions about the timing of the intervention and the process's response. The two most commonly used models within the ITS framework are the autoregressive integrated moving average (ARIMA) (see [18]) and segmented regression (SR) models, referred to as ITS-ARIMA and ITS-SR, respectively. While ITS-SR is widely used, it may not always be effective, especially when seasonality and autocorrelation are present. The ITS-ARIMA model offers an alternative approach that can handle these issues and accommodate more complex effects beyond the basic intervention impact. Many aspects of the design, methods, analysis, and reporting of ITS studies can be improved, particularly description of the statistical methods and approaches to adjust for and estimate autocorrelation. According to [18], ARIMA modelling is considered to be a more flexible tool to evaluate health interventions and model different types of impacts among linear regression and generalized additive models. Also, SR can suffer from aggregation bias, which reduces precision and diminishes the ability to detect clinically significant changes. To address this, [8] introduced a weighted SR method that accounts for variability both among patients within a healthcare facility and across different time points by incorporating weights. [21] pointed out a common mistake found in tutorials and published studies using SR for ITS analysis. According to [21], in SR analysis, researchers should not simply multiply the calendar time variable by an indicator for pre- and post-intervention periods to model the post-intervention segment, as this leads to incorrect estimates of level changes. Instead, they should multiply the intervention indicator by the time elapsed since the inter-

vention began, not by the time since the study started. Therefore, the post-intervention segment should be zero before the intervention and start counting from zero at the time of intervention implementation, rather than counting from the study's start.

ITS designs are widely used to evaluate public health interventions in healthcare settings, clinical trials and epidemiology, as demonstrated in studies by [15], [5],

[13], [19], [12], and [6]. ITS models offer an important understanding of how particular strategies affect trends over a period, using statistical techniques to efficiently examine data before and after an intervention.

[9] reported a notable upward trend in the use of ITS analysis over time, with its health application nearly tripling over the past decade. Multiple statistical techniques exist for analyzing ITS data, and researchers need to consider the data types and verify the assumptions required by each method. This review aims to identify and summarize current methods used in ITS analyses within health research, highlight their strengths and weaknesses, describe their applications in health studies, and pinpoint methodological gaps and challenges.

[17] evaluated the effect of the diabetes Canada dissemination and implementation strategy on population-level prescription rates of blood glucose test strips by the ITS analysis to prescribing trends overall and by drug groups. They gathered all diabetes-related medication and test strip claims from Manitoba and Saskatchewan between January 1, 2000, and September 30, 2015. The main outcome measured was the proportion of the cohort each quarter who received test strips according to the 2013 Diabetes Canada guidelines.

Environmental disasters like wildfires, floods, pandemics, and droughts can cause major disruptions and trauma to affected communities. Children and youth may be especially vulnerable to further educational interruptions. However, assessing the effects of disasters is difficult due to challenges in conducting studies and recruiting participants after such events. [14] created an ITS model with a limited number of time points to evaluate learning loss caused by the COVID-19 pandemic and school closures.

Current approaches assume a fixed interruption point with an immediate effect or exclude data where the intervention effect is not fully

realized. To overcome these issues, [7] developed a robust ITS model that allows for inference on identifying the change point, differences in correlation before and after the intervention, changes in outcome variance pre- and post-intervention, and differences in mean outcomes before and after the intervention.

[20] considered the Durbin-Watson test to detect autocorrelation in the ITS model with different scenarios, including variations in level and slope changes, different time series lengths, and autocorrelation at lag one. They employed several estimation methods, including ordinary least squares, generalized least squares, Newey-West, and restricted maximum likelihood methods.

Due to the lack of addressing the spatiotemporal heterogeneities alongside causal relationships in ITS, [22] introduced a spatially ITS design and examined spatiotemporal heterogeneity patterns in the causal impacts of policy interventions. This approach was used to causally assess how the effects of mobility control policies during the early phase of the COVID-19 outbreak differed across both space and time, utilizing a mobile phone data set from Shenzhen, China. Their modeling results identified and differentiated significant temporal, spatial, and spatiotemporal variations in the causal effects of these policies, (also, see [10]).

The COVID-19 pandemic has severely impacted healthcare systems globally, including organ transplantation. [16] investigated the number of living donor transplants performed in the United States, uncovering a significant pandemic-related decline in donation rates, a 22.6% drop from 2019 to 2020. Their analysis used data on donor transplants from the United Network for Organ Sharing spanning January 2002 to August 2021, applying the ITS model with March 2020 marked as the intervention point. Furthermore, the kidney allocation policy introduced in March 2021 was considered a second intervention event specifically for kidney donor transplants.

In recent decades, significant attention has been directed towards the field of asymmetric and heavy-tailed distributions. One of the earliest alternatives proposed to the normal distribution is the skew normal distribution, which has seen various extensions over time, further enhancing its popularity. [3] introduced the univariate skew normal, which is a subclass of the symmetric normal distribution, whereas the multivari-

ate one was introduced by [4]. A natural direction for extending the normal distribution is the introduction of some sort of skewness, both in the univariate and multivariate settings. The split normal (SN) or two-piece normal distribution originally introduced by [11], such that it results from joining at the mode the corresponding halves of two normal distributions with the same mode but different variances. Recently, [1] proposed a generalized mixture of the normal and derived numerous properties of the proposed family.

All models proposed within the ITS framework have been restricted to symmetric normal distributions. However, in real-world scenarios, we frequently encounter many asymmetric observations, where normal models are less effective in fitting. Therefore, to address this limitation for non-normal phenomena, we focus on examining the behavior of ITS models with asymmetric or heavy-tailed characteristics. Moreover, we consider regime-switching autocorrelation of the ITS model, which is more compatible with real situations. Existing ITS analysis methods do not account for changes in correlation after the intervention, which is a significant limitation. In the present paper, we have addressed both existing issues, as non-normal innovations and regime-switching autocorrelation coefficient, with a comprehensive discussion of the Bayesian estimation of the parameters of the process.

The paper is organized as follows. The basic definition of the SN distribution, the interrupted autoregressive (IAR) model, and the introduction of the new dynamic IAR model with the SN innovations are provided in section 2. The Bayesian estimation of the unknown parameters is the main subject of section 3. The simulation results of the Bayesian estimates are provided in section 4. Finally in section 5, the applicability of the new process in real data analysis is checked by the weekly new COVID-19 cases in Greece.

2 The Split Normal distribution and Interrupted Autoregressive Model

In this section, we briefly review two basic topics: SN distribution and the IAR(1) process from the general intervention models.

2.1 The Split Normal distribution

The probability density function (PDF) of the SN distribution with a location parameter μ is introduced by [2] as follows

$$f_X(x) = \begin{cases} \frac{2}{\sigma_1+\sigma_2}\phi\left(\frac{x-\mu}{\sigma_1}\right), & x < \mu \\ \frac{2}{\sigma_1+\sigma_2}\phi\left(\frac{x-\mu}{\sigma_2}\right), & x \geq \mu \end{cases}, \tag{1}$$

where $\phi(\cdot)$ denotes the standard normal PDF. The notation $\mathrm{SN}(\mu, \sigma_1, \sigma_2)$ denotes a SN distribution with parameters $(\mu, \sigma_1, \sigma_2)$, where $\mu \in (-\infty, \infty)$ and $\sigma_j \in (0, \infty)$ for $j = 1, 2$. The stochastic representation of the SN is given by

$$X = \mu + \sigma W|Z|, \quad \mu \in \mathbb{R}, \sigma > 0,$$

where Z is a standard normal random variable and is independent of W, which is a discrete random variable with the following probability mass function

$$P(W = w) = p(w \mid \gamma) = \gamma^{(1+s)/2}(1-\gamma)^{\frac{1-s}{2}}, \quad w = \gamma, -(1-\gamma), \quad 0 \leq \gamma \leq 1$$

and $s = \mathrm{sgn}(w) = \begin{cases} 1, & w \geq 0 \\ -1, & w < 0 \end{cases}$.

For SN distribution, the following hierarchical representation holds

$$\begin{aligned} X \mid W = w &\sim \phi(x \mid \mu, \sigma^2 w^2)(\mathrm{I}_A(x))^{\frac{1+s}{2}}(\mathrm{I}_{A^c}(x))^{\frac{1-s}{2}}, \\ W &\sim p(w \mid \gamma), \end{aligned}$$

where $A = (\infty, \mu)$ and A^c is the complement of A. Based on the reparameterization $\sigma = \sigma_1 + \sigma_2$ and $\gamma = \frac{\sigma_1}{\sigma_1+\sigma_2}$, by substituting into equation (1), we can write

$$f_X(x) = 2\left(\gamma\phi(x \mid \mu, \sigma^2\gamma^2)\mathrm{I}(x < \mu) + (1-\gamma)\phi(x \mid \mu, \sigma^2(1-\gamma^2))\mathrm{I}(x \geq \mu)\right),$$

where $\mathrm{I}(\cdot)$ is the indicator function.

2.2 The Interrupted Autoregressive Model

Intervention models can be used to describe how an intervention impacts a time series; however, the input series is represented by a simple indicator variable showing whether the event is present or not. In this context, intervention function modeling involves considering the dynamic relationship between two time series. Intervention analysis can be performed to address any abnormal values caused by the intervention event in the series, to estimate the effect of implementing the intervention on a specific outcome, or the intervention effect itself. This approach ensures that the results of the time series analysis, such as the model structure, parameter estimates, and future forecasts, are not significantly distorted by the presence of these unusual values.

For specified values of the delay parameter b and orders p, q, the IAR(1) process is represented as

$$Y_t = \alpha Y_{t-1} + \sum_t f(R_t) + \epsilon_t, \quad \alpha \in (-1, 1),$$

where $f(R_t)$ is the intervention function at time t, defined as $f(R_t) = \frac{\omega(B)}{\delta(B)} B^b R_t$, and $B^b R_t = R_t - R_{t-1} - \ldots - R_{t-b}$ is the backward shift operator, such that

$$\omega(B) = \omega_0 - \omega_1 B - \ldots - \omega_p B^p, \quad \delta(B) = 1 - \delta_1 B - \ldots - \delta_q B^q.$$

The intervention may involve a long-term change, such as adopting lifestyle practice guidelines, or a short-term action, like a product sales promotion. Different intervention functions can be chosen to address various situations, including: an abrupt onset with a long duration, an abrupt onset with a short duration, a gradual onset with a long duration, and a gradual onset followed by a slow decline.

If we use m to indicate the start time of the intervention, the intervention function falls into the categories of step change, pulse, and ramp. The step (level) change referrs a sudden and continuous shift that occurs immediately after an intervention and moves the time series up or down by a certain amount as $R_{1,t} = \begin{cases} 1, & t \geq m \\ 0, & t < m \end{cases}$. The pulse is a sudden, transient shift that occurs for one or more moments immediately following

an intervention before returning to baseline as $R_{2,t} = \begin{cases} 1, & t = m \\ 0, & t \neq m \end{cases}$. Th ramp is a slope change that occurs immediately after the intervention as $R_{3,t} = \begin{cases} t - T_0 + 1, & t \geq m \\ 0, & t < m \end{cases}$, where T_0 represents the starting time for the ramp effect.

2.3 The new DIAR-SN(1) process

In real situations, the autoregressive coefficient may not be constant before and after the intervention, and the innovations do not show any symmetric pattern. Therefore, the classical IAR(1) process cannot handle such cases. Considering the previous shortcomings, we introduce the dynamic step change function of the IAR(1) model with the SN innovations and regime-switching coefficients to overcome all the unique aspects of the real data set.

We consider the dynamic step change function as follows

$$Z_t = \alpha Z_{t-1} + \beta \mathrm{I}_t(m), \qquad \mathrm{I}_t(m) = \begin{cases} 0, & t \leq m \\ 1, & t > m \end{cases},$$

where α and β are the parameters of the intervention effect. Therefore, the IAR(1) intervention process with the dynamic step change component is defined as

$$Y_t = \rho Y_{t-1} + Z_t + \epsilon_t = \rho Y_{t-1} + \alpha Z_{t-1} + \beta \mathrm{I}_t(m) + \epsilon_t,\ \alpha, \rho \in (-1, 1),\ Y_t \in \mathbb{R},\ t \geq 1,$$

the parameter ρ is the autoregressive coefficient and ϵ_t is the innovation. The autoregressive coefficient may change in the two regimes, so we introduce the IAR(1) model with regime-switching autoregressive coefficients as follows

$$Y_t = \begin{cases} \rho_1 Y_{t-1} + \epsilon_t, & t \leq m \\ \rho_2 Y_{t-1} + \alpha Z_{t-1} + \beta + \epsilon_t, & t > m \end{cases},$$

where $\alpha, \rho \in (-1, 1),\ Y_t \in \mathbb{R},\ t \geq 1$.

The proposed IAR(1)process also be expressed as

$$Y_t = (\rho_1 \mathrm{I}_{1,t}(m) + \rho_2 \mathrm{I}_{2,t}(m)) Y_{t-1} + \alpha Z_{t-1} + \beta \mathrm{I}_{2,t}(m) + \epsilon_t,$$

such that $\mathrm{I}_{2,t}(m) = 1 - \mathrm{I}_{1,t}(m) = \mathrm{I}_t(m)$.

By considering $Y_t - \alpha Y_{t-1}$, we have

$$Y_t = (\alpha+\rho_1\mathrm{I}_{1,t}(m)+\rho_2\mathrm{I}_{2,t}(m))Y_{t-1}-\alpha(\rho_1\mathrm{I}_{1,t-1}(m)+\rho_2\mathrm{I}_{2,t-1}(m))Y_{t-2}-\beta\mathrm{I}_{2,t}(m)+\epsilon_t, \tag{2}$$

where $\epsilon_t^* = \epsilon_t - \alpha\epsilon_{t-1}$. We consider that ϵ_t^* follows the SN distribution with parameters $(\mu, \sigma_1, \sigma_2)$. The new dynamic IAR(1) in (2), with the asymmetric innovation of SN distribution, is called DIAR-SN(1) for short, where the parameter vector is represented by $\Delta = (\alpha, \beta, \rho_1, \rho_2, \mu, \sigma_1, \sigma_2)$.

The conditional probability of the proposed process is represented as

$$P(Y_t < j | i_1 \le Y_{t-1} < i_1 + d_1, i_2 \le Y_{t-2} < i_2 + d_2), \quad d_1, d_2 > 0,$$

when $d_1, d_2 \to 0$, it can be concluded that

$$\begin{aligned} P(Y_t < y_t | Y_{t-1} = y_{t-1}, Y_{t-2}) &= \mathrm{I}_{1,t}(m)P(\epsilon_t^* \le y_t - (\alpha+\rho_1)y_{t-1} + \alpha\rho_1 y_{t-2}) \\ &\quad + \mathrm{I}_{2,t}(m)P(\epsilon_t^* \le y_t - (\alpha+\rho_2)y_{t-1} + \alpha\rho_2 y_{t-2} - \beta) \\ &= \mathrm{I}_{1,t}(m)F_{\epsilon_t^*}(y_t - (\alpha+\rho_1)y_{t-1} + \alpha\rho_1 y_{t-2}) \\ &\quad + \mathrm{I}_{2,t}(m)F_{\epsilon_t^*}(y_t - (\alpha+\rho_2)y_{t-1} + \alpha\rho_2 y_{t-2} - \beta), \end{aligned}$$

where $F_{\epsilon_t^*}(\cdot)$ is the CDF of the SN. Consequently, the conditional PDF of the DIAR-SN(1) process is represented as follows

$$\begin{aligned} f(y_t | y_{t-1}, y_{t-2}) &= \mathrm{I}_{1,t}(m) f_{\epsilon_t^*}(y_t - (\alpha+\rho_1)y_{t-1} + \alpha\rho_1 y_{t-2}) \\ &+ \mathrm{I}_{2,t}(m) f_{\epsilon_t^*}(y_t - (\alpha+\rho_2)y_{t-1} + \alpha\rho_2 y_{t-2} - \beta), \end{aligned}$$

where $f_{\epsilon_t^*}(\cdot)$ is the PDF of the SN distribution. If we set, $\sigma = \sigma_1 + \sigma_2$ and $\gamma = \frac{\sigma_i}{\sigma_1+\sigma_2}$, then

$$f_{\epsilon_t^*}(\epsilon) = 2\left[\gamma\phi(\epsilon|0, \sigma^2\gamma^2)\mathrm{I}(\epsilon < 0) + (1-\gamma)\phi(\epsilon|0, \sigma^2(1-\gamma)^2)\mathrm{I}(\epsilon \ge 0)\right].$$

For ease of calculations, we consider $\mu = 0$.

3 The Bayesian Estimation of the Unknown Parameters

This section explains the procedure for estimating the unknown parameters of the DIAR-SN(1) process using observed data $Y_1, Y_2, \ldots, Y_T$. To

estimate these parameters, we employed the MCMC method within a Bayesian framework.

3.1 Augmented-likelihood Function

Additional notation is introduced to derive the augmented likelihood function from the DIAR-SN(1) model, followed by posterior analysis using random samples. Let $C_t = (Y_t, W_t),\ t = 1, \ldots, T$ represent the complete data, where $Y_1, \ldots, Y_T$ are independent and identically distributed (i.i.d.) variables from the DIAR-SN(1) process, and $W_1, \ldots, W_T$ are i.i.d. latent random variables. The vector of parameters is denoted as $\Delta = (\alpha, \beta, \rho_1, \rho_2, \sigma, \gamma)$. Using the hierarchical model representation along with vectors $W = (W_1, \ldots, W_T)'$ and $Y = (Y_1, \ldots, Y_T)'$, we obtain

$$Y_t|W_t = w_t \sim \phi(y_t - (\alpha+\rho_1)y_{t-1} + \alpha\rho_1 y_{t-2}|0, \sigma^2 w^2)\Big(\mathrm{I}_{A_1}(y_t)\Big)^{\frac{1+s}{2}}\Big(\mathrm{I}_{A_1^c}(y_t)\Big)^{\frac{1-s}{2}},$$

for $t = 1, \ldots, m-1$,

$$Y_t|W_t = w_t \sim \phi(y_t - (\alpha+\rho_2)y_{t-1} + \alpha\rho_2 y_{t-2} - \beta|0, \sigma^2 w^2)\Big(\mathrm{I}_{A_2}(y_t)\Big)^{\frac{1+s}{2}}\Big(\mathrm{I}_{A_2^c}(y_t)\Big)^{\frac{1-s}{2}},$$

and $W_t \sim p(w_t|\gamma)$, for $t = m, \ldots, T$, where,

$$\mathrm{I}_{A_1}(y_t) = \begin{cases} 1, & y_t \geq (\alpha+\rho_1)y_{t-1} - \alpha\rho_1 y_{t-2}, \\ 0, & \text{o.w.} \end{cases}$$

$$\mathrm{I}_{A_2}(y_t) = \begin{cases} 1, & y_t \geq (\alpha+\rho_2)y_{t-1} - \alpha\rho_2 y_{t-2} + \beta, \\ 0, & \text{o.w.} \end{cases}$$

The augmented-likelihood function is represented as follows

$$
\begin{aligned}
L\left(\Delta, C\right) &= \prod_{t=2}^{T} P(W_t = w_t) f\left(Y_t | W_t, Y_{t-1}, Y_{t-2}\right) \qquad (3)\\
&= \gamma^{\frac{T}{2}+\frac{1}{2}\sum_{t=1}^{T} s_t} (1-\gamma)^{\frac{T}{2}-\frac{1}{2}\sum_{t=1}^{T} s_t} \prod_{t=2}^{m-1} \phi\left(y_t - (\alpha+\rho_1) y_{t-1} + \alpha\rho_1 y_{t-2} | 0, \sigma^2 w_t^2\right)\\
&\quad \prod_{t=m}^{T} \phi\left(y_t - (\alpha+\rho_2) y_{t-1} + \alpha\rho_2 y_{t-2} - \beta | 0, \sigma^2 w_t^2\right) \mathrm{I}_{(Y^-, Y^+)}(0)\\
&= \gamma^{\frac{T}{2}+\frac{1}{2}\sum_{t=1}^{T} s_t} (1-\gamma)^{\frac{T}{2}-\frac{1}{2}\sum_{t=1}^{T} s_t} \prod_{t=2}^{T} \frac{1}{\sqrt{2\pi\sigma^2 w_t^2}} \qquad (4)\\
&\quad \exp\Big(\sum_{t=2}^{m-1} \frac{-\left(y_t - (\alpha+\rho_1) y_{t-1} + \alpha\rho_1 y_{t-2}\right)^2}{2\sigma^2 w_t^2}\Big)\\
&\quad \exp\Big(\sum_{t=m}^{T} \frac{-\left(y_t - (\alpha+\rho_2) y_{t-1} + \alpha\rho_2 y_{t-2} - \beta\right)^2}{2\sigma^2 w_t^2}\Big) \mathrm{I}_{(Y^-, Y^+)}(0),
\end{aligned}
$$

where $Y^- = \max\{Y_t; W_t = -(1-\gamma)\}$ and $Y^+ = \min\{Y_t; W_t = \gamma\}$. Ignoring constants, the augmented log-likelihood function is expressed as follows

$$
\begin{aligned}
\ell\left(\Delta, C\right) \quad \propto \quad & \Big(\frac{T}{2} + \frac{1}{2}\sum_{t=1}^{T} s_t\Big) \ln(\gamma) + \Big(\frac{T}{2} - \frac{1}{2}\sum_{t=1}^{T} s_t\Big) \ln(1-\gamma) + \frac{T}{2}\ln(\sigma^2)\\
& - \sum_{t=2}^{m-1} \frac{\left(y_t - (\alpha+\rho_1) y_{t-1} + \alpha\rho_1 y_{t-2}\right)^2}{2\sigma^2 w_t^2} \qquad (5)\\
& - \sum_{t=m}^{T} \frac{\left(y_t - (\alpha+\rho_2) y_{t-1} + \alpha\rho_2 y_{t-2} - \beta\right)^2}{2\sigma^2 w_t^2}.
\end{aligned}
$$

3.2 Prior Distributions of the Parameters of the DIAR-SN(1) Process

When there is no prior information or previous experiments regarding the parameters, non-informative prior distributions are used. Here, the independent priors of the parameters of DIAR-SN(1) process Δ are specified as

$$\alpha \sim \mathrm{TN}_{(-1,1)}(\nu_1, \kappa_1^2), \qquad \rho_1 \sim \mathrm{TN}_{(-1,1)}(\nu_2, \kappa_2^2), \qquad \rho_2 \sim \mathrm{TN}_{(-1,1)}(\nu_3, \kappa_3^2),$$
$$\beta \sim \mathrm{N}(\nu_4, \kappa_4^2), \qquad \gamma \sim \mathrm{Beta}(a_1, b_1), \qquad \sigma^2 \sim \mathrm{IG}(a_2, b_2),$$

where a_i, b_i, $i = 1, 2$ and ν_i, κ_i, $i = 1, \ldots, 4$, are known hyperparameters, and TN, Beta, and IG imply the truncated normal, Beta and inverse-gamma distributions, respectively. The joint prior distribution for Δ is represented as

$$\pi(\Delta) = \Big(\frac{1}{\sqrt{2\pi\kappa_1^2}}\Big) \frac{\exp\big(\frac{-(\alpha-\nu_1)^2}{2\kappa_1^2}\big)}{\Phi(\frac{1-\nu_1}{\kappa_1}) - \Phi(\frac{-1-\nu_1}{\kappa_1})} \Big(\frac{1}{\sqrt{2\pi\kappa_2^2}}\Big) \frac{\exp\big(\frac{-(\rho_1-\nu_2)^2}{2\kappa_2^2}\big)}{\Phi(\frac{1-\nu_2}{\kappa_2}) - \Phi(\frac{-1-\nu_2}{\kappa_2})} \Big(\frac{1}{\sqrt{2\pi\kappa_3^2}}\Big)$$

$$\frac{\exp\big(\frac{-(\rho_2-\nu_3)^2}{2\kappa_3^2}\big)}{\Phi(\frac{1-\nu_3}{\kappa_3}) - \Phi(\frac{-1-\nu_3}{\kappa_3})} \Big(\frac{1}{\sqrt{2\pi\kappa_4^2}}\Big) \exp\big(\frac{-(\beta-\nu_4)^2}{2\kappa_4^2}\big)$$

$$\frac{\Gamma(a_1+b_1)}{\Gamma(a_1)\Gamma(b_1)} \gamma^{a_1-1}(1-\gamma)^{b_1-1} \frac{a_2^{b_2}}{\gamma(a_2)} \Big(\frac{1}{\sigma^2}\Big)^{a_2+1} \exp\big(\frac{-b_2}{\sigma^2}\big).$$

3.3 Posterior Distributions of the Parameters of the DIAR-SN(1) Process

By combining the augmented likelihood function (3) with the independent prior distributions $\pi(\Delta)$, the full joint posterior distribution is derived as follows

$$\pi\big(\Delta, W|Y\big) \propto L(\Delta, C)\pi(\Delta) \tag{6}$$

Since the posterior distribution (6) cannot be solved analytically, samples are drawn from it using the Gibbs sampler within the MCMC framework. Consequently, the marginal posterior distributions of the latent

variables and parameters are obtained in the following. The conditional distributions of the latent variables $W_t, t = 1, \ldots, T$ for the Gibbs sampling are given by $W_t|\Delta, Y = \begin{cases} -(1-\gamma), & Y_t < 0, \\ \gamma, & Y_t > 0, \end{cases}$.

Considering $\Delta_{(-j)}$, which is the parameter vector excluding the j-th element, the conditional posterior distributions of the DIAR-SN(1) parameters with the proposed priors are calculated as stated in the Corollary 3.1 to Corollary 3.6.

Corollary 3.1. *Assuming Y is derived from the DIAR-SN(1) process, the marginal posterior distribution of the unknown parameter α is given by $\alpha|\Delta_{(-\alpha)}, W, Y \sim TN_{(-1,1)}(M_1, S_1)$, where $M_1 = \dfrac{B_1\kappa_1^2 + A_1^2\nu_1}{A_1^2 + \kappa_1^2}$, and $S_1 = \dfrac{A_1^2\kappa_1^2}{A_1^2 + \kappa_1^2}$, such that*

$$A_1^2 = \frac{\sigma^2}{\sum_{t=2}^{m-1} w_t^{-2}(y_{t-1} - \rho_1 y_{t-2})^2 + \sum_{t=m}^{T} w_t^{-2}(y_{t-1} - \rho_2 y_{t-2})^2},$$

$$B_1 = \frac{\sum_{t=2}^{m-1} w_t^{-2}(y_{t-1} - \rho_1 y_{t-2})(y_t - \rho_1 y_{t-1}) + \sum_{t=m}^{T} w_t^{-2}(y_{t-1} - \rho_2 y_{t-2})(y_t - \rho_2 y_{t-1} - \beta)}{\sum_{t=2}^{m-1} w_t^{-2}(y_{t-1} - \rho_1 y_{t-2})^2 + \sum_{t=m}^{T} w_t^{-2}(y_{t-1} - \rho_2 y_{t-2})^2}.$$

Proof. The posterior of the parameter α is obtained as

$$\begin{aligned}
\pi\big(\alpha|\Delta_{(-\alpha)},W,Y\big) &= \frac{\pi\big(\Delta,W|Y\big)}{\pi\big(\Delta_{(-\alpha)},W|Y\big)} = \frac{\pi\big(\Delta,W|Y\big)}{\int_{-1}^{1}\pi\big(\Delta,W|Y\big)\,\mathrm{d}\alpha} \\
&= \frac{\exp\big(\frac{-(\alpha-\nu_1)^2}{2\kappa_1^2}\big)\exp\Big(\sum\limits_{t=2}^{m-1}\frac{-H_1}{2\sigma^2w_t^2}\Big)\exp\Big(\sum\limits_{t=m}^{T}\frac{-H_2}{2\sigma^2w_t^2}\Big)}{\int_{-1}^{1}\exp\big(\frac{-(\alpha-\nu_1)^2}{2\kappa_1^2}\big)\exp\Big(\sum\limits_{t=2}^{m-1}\frac{-H_1}{2\sigma^2w_t^2}\Big)\exp\Big(\sum\limits_{t=m}^{T}\frac{-H_2}{2\sigma^2w_t^2}\Big)\,\mathrm{d}\alpha} \\
&= \frac{\exp\big(\frac{-(\alpha-\nu_1)^2}{2\kappa_1^2}\big)\exp\big(\frac{-(\alpha-B_1)^2}{2A_1^2}\big)}{\int_{-1}^{1}\exp\big(\frac{-(\alpha-\nu_1)^2}{2\kappa_1^2}\big)\exp\big(\frac{-(\alpha-B_1)^2}{2A_1^2}\big)\,\mathrm{d}\alpha} \\
&= \Big(\frac{1}{\sqrt{2\pi S_1^2}}\Big)\frac{\exp\big(\frac{-(\alpha-M_1)^2}{2S_1^2}\big)}{2\Phi(\frac{1}{S_1})-1},
\end{aligned}$$

where $H_1=(y_t-(\alpha+\rho_1)y_{t-1}+\alpha\rho_1y_{t-2})^2$ and $H_2=(y_t-(\alpha+\rho_2)y_{t-1}+\alpha\rho_2y_{t-2}-\beta)^2$. The last equality corresponds to the PDF of a truncated normal distribution bounded between (-1,1) with parameters M_1 and S_1, thus completing the proof. □

Corollary 3.2. *Assuming Y is derived from the DIAR-SN(1) process, the marginal posterior distribution of the unknown parameter ρ_1 is given by $\rho_1|\Delta_{(-\rho_1)},W,Y\sim TN_{(-1,1)}\Big(M_2,S_2\Big)$, where $M_2=\dfrac{B_2\kappa_2^2+A_2^2\nu_2}{A_2^2+\kappa_2^2}$, and $S_2=\dfrac{A_2^2\kappa_2^2}{A_2^2+\kappa_2^2}$, such that*

$$A_2^2=\frac{\sigma^2}{\sum\limits_{t=2}^{m-1}w_t^{-2}(y_{t-1}-\alpha y_{t-2})^2},\qquad B_2=\frac{\sum\limits_{t=2}^{m-1}w_t^{-2}(y_{t-1}-\alpha y_{t-2})(y_t-\alpha y_{t-1})}{\sum\limits_{t=2}^{m-1}w_t^{-2}(y_{t-1}-\alpha y_{t-2})^2}.$$

Proof. The posterior of the parameter ρ_1 is obtained as

$$\begin{aligned}
\pi\big(\rho_1|\Delta_{(-\rho_1)},W,Y\big) &= \frac{\pi\big(\Delta,W|Y\big)}{\pi\big(\Delta_{(-\rho_1)},W|Y\big)} \\
&= \frac{\exp\big(\frac{-(\rho_1-\nu_2)^2}{2\kappa_2^2}\big)\exp\Big(\sum_{t=2}^{m-1}\frac{-H_1}{2\sigma^2 w_t^2}\Big)}{\int_{-1}^{1}\exp\big(\frac{-(\rho_1-\nu_2)^2}{2\kappa_2^2}\big)\exp\Big(\sum_{t=2}^{m-1}\frac{-H_1}{2\sigma^2 w_t^2}\Big)\,\mathrm{d}\rho_1} \\
&= \frac{\exp\big(\frac{-(\rho_1-\nu_2)^2}{2\kappa_2^2}\big)\exp\big(\frac{-(\rho_1-B_2)^2}{2A_2^2}\big)}{\int_{-1}^{1}\exp\big(\frac{-(\rho_1-\nu_2)^2}{2\kappa_2^2}\big)\exp\big(\frac{-(\rho_1-B_2)^2}{2A_2^2}\big)\,\mathrm{d}\rho_1} \\
&= \Big(\frac{1}{\sqrt{2\pi S_2^2}}\Big)\frac{\exp\big(\frac{-(\rho_1-M_2)^2}{2S_2^2}\big)}{2\Phi(\frac{1}{S_2})-1}.
\end{aligned}$$

The last equality corresponds to the PDF of a truncated normal distribution bounded between (-1,1) with parameters M_2 and S_2, thus completing the proof. □

Corollary 3.3. *Assuming Y is derived from the DIAR-SN(1) process, the marginal posterior distribution of the unknown parameter ρ_2 is given by* $\rho_2|\Delta_{(-\rho_2)},W,Y \sim TN_{(-1,1)}\Big(M_3,S_3\Big)$, *where* $M_3=\dfrac{B_3\kappa_3^2+A_3^2\nu_3}{A_3^2+\kappa_3^2}$, *and* $S_3=\dfrac{A_3^2\kappa_3^2}{A_3^2+\kappa_3^2}$, *such that*

$$A_3^2=\frac{\sigma^2}{\sum_{t=m}^{T} w_t^{-2}(y_{t-1}-\alpha y_{t-2})^2},$$

$$B_3=\frac{\sum_{t=m}^{T} w_t^{-2}(y_{t-1}-\alpha y_{t-2})(y_t-\alpha y_{t-1}-\beta)}{\sum_{t=m}^{T} w_t^{-2}(y_{t-1}-\alpha y_{t-2})^2}.$$

Proof. The posterior of the parameter ρ_2 is obtained as

$$\begin{aligned}
\pi\big(\rho_2|\Delta_{(-\rho_2)},W,Y\big) &= \frac{\pi\big(\Delta,W|Y\big)}{\pi\big(\Delta_{(-\rho_2)},W|Y\big)} \\
&= \frac{\exp\big(\frac{-(\rho_2-\nu_3)^2}{2\kappa_3^2}\big)\exp\Big(\sum\limits_{t=m}^{T}\frac{-H_2}{2\sigma^2w_t^2}\Big)}{\int_{-1}^{1}\exp\big(\frac{-(\rho_2-\nu_3)^2}{2\kappa_3^2}\big)\exp\Big(\sum\limits_{t=m}^{T}\frac{-H_2}{2\sigma^2w_t^2}\Big)\,\mathrm{d}\rho_2} \\
&= \frac{\exp\big(\frac{-(\rho_2-\nu_3)^2}{2\kappa_3^2}\big)\exp\big(\frac{-(\rho_2-B_3)^2}{2A_3^2}\big)}{\int_{-1}^{1}\exp\big(\frac{-(\rho_2-\nu_3)^2}{2\kappa_3^2}\big)\exp\big(\frac{-(\rho_2-B_3)^2}{2A_3^2}\big)\,\mathrm{d}\rho_2} \\
&= \Big(\frac{1}{\sqrt{2\pi S_3^2}}\Big)\frac{\exp\big(\frac{-(\rho_2-M_3)^2}{2S_3^2}\big)}{2\Phi(\frac{1}{S_3})-1}.
\end{aligned}$$

The last equality corresponds to the PDF of a truncated normal distribution bounded between (-1,1) with parameters M_3 and S_3, thus completing the proof. □

Corollary 3.4. *Assuming Y is derived from the DIAR-SN(1) process, the marginal posterior distribution of the unknown parameter β is given by $\beta|\Delta_{(-\beta)},W,Y \sim N\Big(M4,S4\Big)$, where $M_4=\dfrac{B_4\kappa_4^2+A_4^2\nu_4}{A_4^2+\kappa_4^2}$, and $S_4=\dfrac{A_4^2\kappa_4^2}{A_4^2+\kappa_4^2}$, such that*

$$A_4^2=\frac{\sigma^2}{\sum\limits_{t=m}^{T}w_t^{-2}},\qquad B_4=\frac{\sum\limits_{t=m}^{T}w_t^{-2}(y_t-(\alpha+\rho_2)y_{t-1}+\alpha\rho_2y_{t-2})}{\sum\limits_{t=m}^{T}w_t^{-2}}.$$

Proof. The posterior of the parameter β is obtained as

$$\begin{aligned}
\pi\big(\beta|\Delta_{(-\beta)},W,Y\big) &= \frac{\pi\big(\Delta,W|Y\big)}{\pi\big(\Delta_{(-\beta)},W|Y\big)} \\
&= \frac{\exp\big(\frac{-(\beta-\nu_4)^2}{2\kappa_4^2}\big)\exp\Big(\sum\limits_{t=m}^{T}\frac{-H_2}{2\sigma^2 w_t^2}\Big)}{\int_{-\infty}^{\infty}\exp\big(\frac{-(\beta-\nu_4)^2}{2\kappa_4^2}\big)\exp\Big(\sum\limits_{t=m}^{T}\frac{-H_2}{2\sigma^2 w_t^2}\Big)\,\mathrm{d}\alpha} \\
&= \frac{\exp\big(\frac{-(\beta-\nu_4)^2}{2\kappa_4^2}\big)\exp\big(\frac{-(\beta-B_4)^2}{2A_1 4^2}\big)}{\int_{-\infty}^{\infty}\exp\big(\frac{-(\beta-\nu_4)^2}{2\kappa_4^2}\big)\exp\big(\frac{-(\beta-B_4)^2}{2A_4^2}\big)\,\mathrm{d}\beta} \\
&= \Big(\frac{1}{\sqrt{2\pi S_4^2}}\Big)\exp\big(\frac{-(\beta-M_4)^2}{2S_4^2}\big).
\end{aligned}$$

The last corresponds to the PDF of a truncated normal distribution bounded between (-1,1) with parameters M_4 and S_4, thus completing the proof. □

Corollary 3.5. *Assuming Y is derived from the DIAR-SN(1) process, the marginal posterior distribution of the unknown parameter γ is given as* $\gamma|\Delta_{(-\gamma)},W,Y \sim Beta\Big(a_1+\frac{T}{2}+\frac{1}{2}\sum_{t=1}^{T}s_t, b_1+\frac{T}{2}-\frac{1}{2}\sum_{t=1}^{T}s_t\Big)$.

Proof. The posterior of the parameter γ is obtained as

$$\begin{aligned}
\pi\big(\gamma|\Delta_{(-\gamma)},W,Y\big) &= \frac{\pi\big(\Delta,W|Y\big)}{\pi\big(\Delta_{(-\gamma)},W|Y\big)} \\
&= \frac{\gamma^{a_1+\frac{T}{2}+\frac{1}{2}\sum_{t=1}^{T}s_t-1}(1-\gamma)^{b_1+\frac{T}{2}-\frac{1}{2}\sum_{t=1}^{T}s_t-1}}{\int_0^1 \gamma^{a_1+\frac{T}{2}+\frac{1}{2}\sum_{t=1}^{T}s_t-1}(1-\gamma)^{b_1+\frac{T}{2}-\frac{1}{2}\sum_{t=1}^{T}s_t-1}\,\mathrm{d}\gamma} \\
&= \frac{1}{B(a_1+\frac{T}{2}+\frac{1}{2}\sum_{t=1}^{T}s_t, b_1+\frac{T}{2}-\frac{1}{2}\sum_{t=1}^{T}s_t)}\gamma^{a_1+\frac{T}{2}+\frac{1}{2}\sum_{t=1}^{T}s_t-1} \\
&\quad (1-\gamma)^{b_1+\frac{T}{2}-\frac{1}{2}\sum_{t=1}^{T}s_t-1},
\end{aligned}$$

where $B(a,b)=\frac{\Gamma(a)\Gamma(b)}{\Gamma(a+b)}$ is the Beta function. The last equality is the PDF of the Beta distribution with parameters $a_1+\frac{T}{2}+\frac{1}{2}\sum_{t=1}^{T}s_t$ and $b_1+\frac{T}{2}-\frac{1}{2}\sum_{t=1}^{T}s_t$, which completes the proof. □

Corollary 3.6. Assuming Y is derived from the DIAR-SN(1) process, the marginal posterior distribution of the unknown parameter σ^2 is given as $\sigma^2|\Delta_{(-\sigma^2)},W,Y\sim \mathrm{IG}\Big(a_2+\frac{T}{2}, b_2+\sum_{t=2}^{m-1}\frac{H_1^2}{2w_t^2}+\sum_{t=m}^{T}\frac{H_2^2}{2w_t^2}\Big)$.

Proof. The posterior of the parameter σ^2 is obtained as

$$\begin{aligned}
\pi\big(\sigma^2|\Delta_{(-\sigma^2)},W,Y\big) &= \frac{\pi\big(\Delta,W|Y\big)}{\pi\big(\Delta_{(-\sigma^2)},W|Y\big)} = \frac{\pi\big(\Delta,W|Y\big)}{\int_0^\infty \pi\big(\Delta,W|Y\big)\,\mathrm{d}\sigma^2} \\
&= \frac{(\sigma^2)^{-(\frac{T}{2}+a_2+1)}\exp\Big(\frac{-1}{\sigma^2}\Big(b_2+\sum_{t=2}^{m-1}\frac{H_1}{2w_t^2}+\sum_{t=m}^{T}\frac{H_2}{2w_t^2}\Big)\Big)}{\int_0^\infty(\sigma^2)^{-(\frac{T}{2}+a_2+1)}\exp\Big(\frac{-1}{\sigma^2}\Big(b_2+\sum_{t=2}^{m-1}\frac{H_1}{2w_t^2}+\sum_{t=m}^{T}\frac{H_2}{2w_t^2}\Big)\Big)\,\mathrm{d}\sigma^2} \\
&= \frac{\Big(b_2+\sum_{t=2}^{m-1}\frac{H_1}{2w_t^2}+\sum_{t=m}^{T}\frac{H_2}{2w_t^2}\Big)^{a_2+\frac{T}{2}}}{\Gamma\Big(\frac{T}{2}+a_2\Big)}(\sigma^2)^{-(\frac{T}{2}+a_2+1)} \\
&\quad \exp\Big(\frac{-1}{\sigma^2}\Big(b_2+\sum_{t=2}^{m-1}\frac{H_1}{2w_t^2}+\sum_{t=m}^{T}\frac{H_2}{2w_t^2}\Big)\Big).
\end{aligned}$$

The last equality is the PDF of the inverse-gamma distribution with parameters $a_2+\frac{T}{2}$ and $b_2+\sum_{t=2}^{m-1}\frac{H_1}{2w_t^2}+\sum_{t=m}^{T}\frac{H_2}{2w_t^2}$, which completes the proof. □

4 Simulation Comparison Results

In this section we present the Monte Carlo Markov Chain (MCMC) simulation results of the DIAR-SN(1) model, which has been conducted to evaluate the performance of the Bayesian estimates for two combinations of parameters as follows

Case one:	$\alpha=0.3$	$\rho_1=0.7$	$\rho_2=0.2$	$\beta=2$	$\sigma=0.8$	$\gamma=0.25$
Case Two:	$\alpha=0.7$	$\rho_1=0.4$	$\rho_2=0.6$	$\beta=1.5$	$\sigma=0.6$	$\gamma=0.42$

The chosen parameter values serve solely to evaluate the effectiveness of the proposed method. The hyperparameters of the prior distributions

were set close to the true values to facilitate faster convergence of the algorithm.

The sample path plot of the DIAR-SN(1) process is shown in Figure 1, for cases one and two of parameters with n=200 sample size. In the first case, the difference between the two regimes before and after the intervention is trivial, while in the second case, the difference is impressive.

Using a sample size of $T = 100, 200, 500, 1000$, along with $H = 1000$ iterations of the MCMC simulation, the Bayesian estimates and root mean square errors (RMSE) of the two cases of the parameters are summarized in Table 1 and Table 2, which indicates the convergency of the Bayesian estimates to real values of the parameters of the DIAR-SN(1) process.

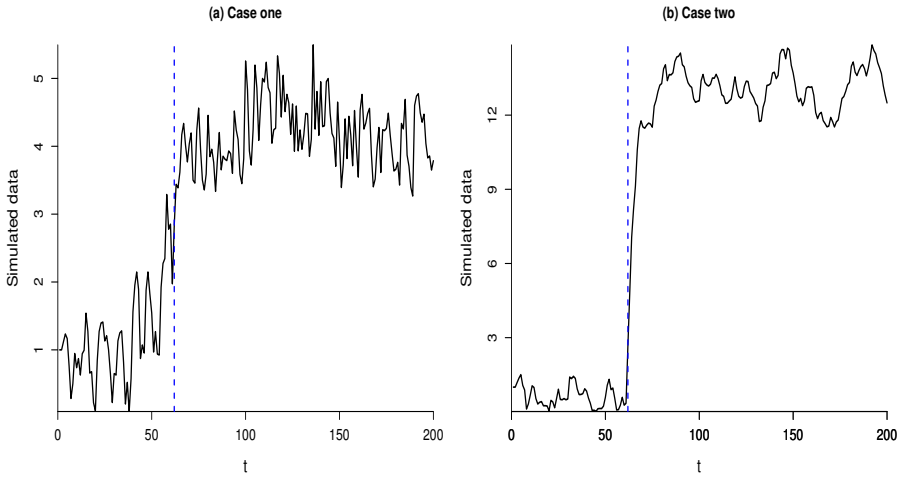

Figure 1: Time series plots of the parameters chain in MCMC.

The Gibbs sampling chains is the plots of iteration number versus the cumulative mean of samples up to each iteration. The Gibbs chain of cases one and two are respectively provided in Figure 2 and Figure 3, which show good mixing.

The posterior densities of the parameters in cases one and two are respectively illustrated in Figure 4 and Figure 5, demonstrating the pos-

Table 1: Estimation of the DIAR-SN(1) model and RMSE in brackets, under case one.

n	$\hat{\alpha}$	$\hat{\rho}_1$	$\hat{\rho}_2$	$\hat{\beta}$	$\hat{\sigma}$	$\hat{\gamma}$
100	0.28269	0.72427	0.20841	2.09658	0.837551	0.25909
St. err.	(0.03969)	(0.10644)	(0.01719)	(0.22524)	(0.11402)	(0.02436)
200	0.30533	0.690204	0.20154	2.078298	0.778154	0.25768
St. err.	(0.03408)	(0.09078)	(0.01097)	(0.20140)	(0.11048)	(0.01343)
500	0.29092	0.70681	0.19763	2.312318	0.78209	0.24965
St. err.	(0.02146)	(0.07121)	(0.00894)	(0.14262)	(0.08245)	(0.00928)
1000	0.29608	0.70266	0.19952	2.42879	0.78894	0.25014
St. err.	(0.00818)	(0.05779)	(0.00557)	(0.08931)	(0.06885)	(0.00675)

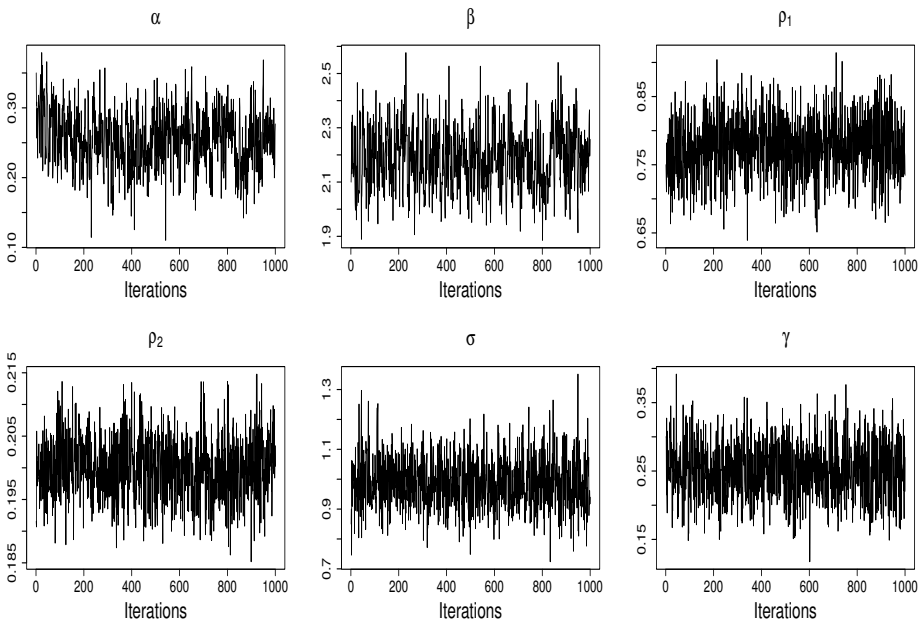

Figure 2: Time series plots of the parameters chain in MCMC for case one.

Table 2: Estimation of the DIAR-SN(1) model and RMSE in brackets, under case two.

n	$\hat{\alpha}$	$\hat{\rho}_1$	$\hat{\rho}_2$	$\hat{\beta}$	$\hat{\sigma}$	$\hat{\gamma}$
100	0.67555	0.41809	0.62149	1.55839	0.58027	0.40402
St. err.	(0.09671)	(0.04903)	(0.08111)	(0.18898)	(0.05398)	(0.04701)
200	0.68255	0.38929	0.607565	1.54553	0.58566	0.415603
St. err.	(0.08025)	(0.04748)	(0.06279)	(0.14536)	(0.04876)	(0.04265)
500	0.69140	0.39187	0.69318	1.52091	0.59348	0.423179
St. err.	(0.06298)	(0.02805)	(0.05116)	(0.10164)	(0.04029)	(0.03398)
1000	0.69647	0.39678	0.69709	1.51713	0.59621	0.42156
St. err.	(0.05386)	(0.01311)	(0.04868)	(0.08625)	(0.03499)	(0.02297)

terior distribution shapes, with smooth, symmetric curves suggesting well-behaved estimates.

5 Real Data Analysis

We considered weekly new COVID-19 cases in Greece from 01/03/2020 to 17/12/2023 (T=199). In Greece, the immunization and vaccination program started on 28 December 2020, and the first booster doses of the vaccine were administered on 14 September 2021. The booster dose significantly reduced the number of COVID-19 cases. The sample trajectory of COVID-19 cases is presented in Figure 6, showing two different regimens before and after $t = 101$. It can be seen that as the booster dose of the COVID-19 vaccine was administered, the number of new COVID-19 cases decreased. In fact, new cases detected decreased, and the efficacy of the booster dose was observed within 6 weeks.

Some statistical measures of the COVID-19 dataset are summarized in Table 3. Thus, the COVID-19 data is right-skewed, leptokurtic (fat tails), and has outliers.

The Bayesian estimates of the unknown parameters of the model under COVID-19 data set are provided in Table 4.

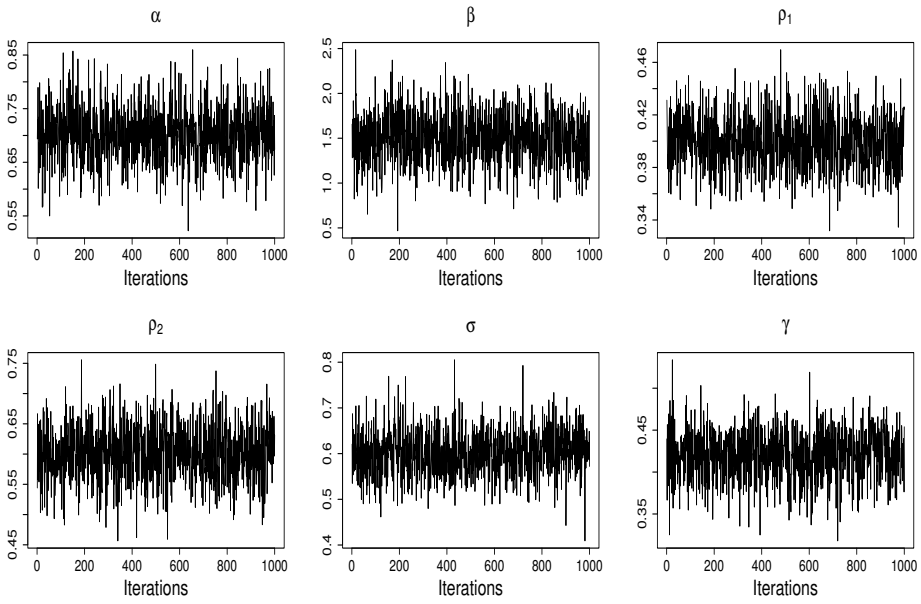

Figure 3: Time series plots of the parameters chain in MCMC for case two.

Table 3: Statistical measurements of the COVID-19 Dataset

Kurtosis	Skewness	Standard Deviation	mean
9.680243	2.490094	39809.9	27808.86

6 Summary and Conclusion

The classical time series models like ARIMA and IARIMA do not effectively capture the nonlinear or stochastic nature of the autoregressive coefficient structure found in the dataset. Additionally, both classical models rely on the assumption of a symmetric normal distribution, which real-world events often violate. This paper aimed to overcome these limitations by developing a new IAR process that incorporates the autoregressive coefficients of the regime variable, SN innovations, and an intervention variable treated as an exogenous factor. The unknown parameters were estimated using the Bayesian approach based on the DIAR-SN(1) process, and these Bayesian estimates converged closely to the true parameter values. The theoretical findings were validated us-

Table 4: The Bayesian estimates of the COVID-19 Dataset under the DIAR-SN(1) model.

Parameters	α	ρ_1	ρ_2	β	γ	σ
Bayesian estimates	0.875	0.299	0.707	1.801	0.633	28472.4

ing two methods: simulated data and real-world datasets. A notable observation was that the Christmas holidays and non-compliance with quarantine measures led to a sudden spike in infection numbers. It was also inferred that the number of new cases began to decline concurrently with the rollout of the COVID-19 booster dose, with the booster's effectiveness becoming apparent approximately six weeks after its implementation.

Future research could explore several areas, including the benefits of the Bayesian approach and its application to modeling high-dimensional data, which may offer effective solutions in regression modeling. Sug-

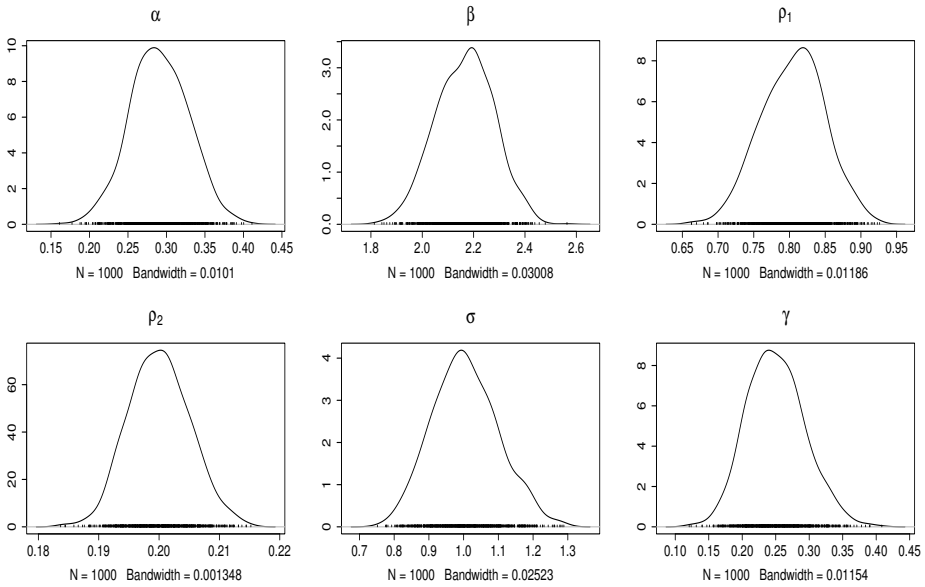

Figure 4: Posterior densities of the parameters for case one.

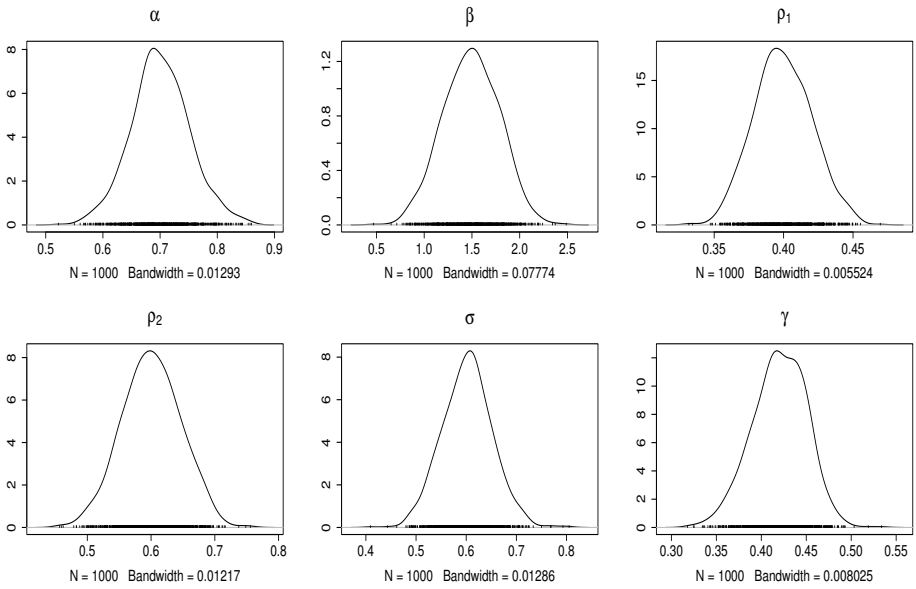

Figure 5: Posterior densities of the parameters for case two.

gested directions for further studies include:

- Computing E-Bayes estimators for the parameters of the DIAR-SN(1) distribution under various loss functions and informative prior distributions. - Exploring other statistical models within the DIAR-SN(1) distribution family.
- Applying the DIAR-SN(1) asymmetric distribution family to model censored data.
- Developing a discrete version of the DIAR-SN(1) distribution through different discretization techniques and assessing the performance of this new discrete distribution in modeling discrete data.

Data availability statements

The data that support the findings of this study and the software code are available from the corresponding author upon reasonable request.

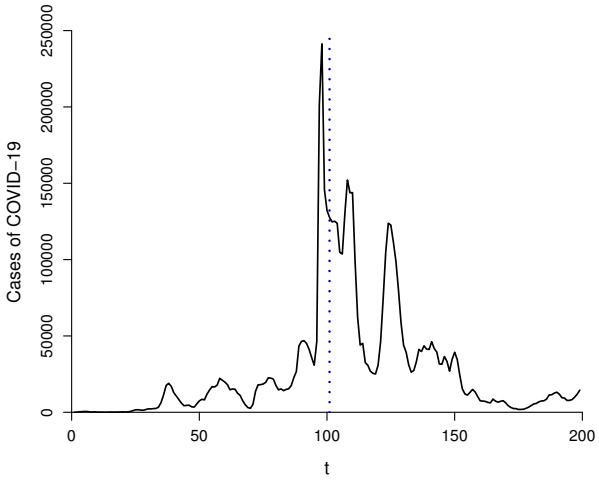

Figure 6: Sample path plot of the COVID-19.

Figure 7: Please write your figure caption here

Example 6.1. Check out our amazing numerical example. Check results in Table 1.

Manuscripts of papers intended for publication should be prepared according to the instruction and submitted through the electronic Journal system by understanding that they have not been published, submitted or accepted for publication elsewhere. The manuscript should be written in English language. Authors are invited to submit their papers as PDF and Tex files using the Journal System for online manuscript submission and management. The authors will be asked to supply the title of the paper, abstract, keywords and AMS classification, and to suggest of the Editorial Board whose area lies closest to the subject. Every manuscript considered for publication is passed to referees for peer review, and then it is subject to final approval by the Editorial Board. After the paper has been accepted, the author(s) are asked to provide the source in LaTeX format together with all accompanying files, ac-

cording to the guidelines. The manuscripts must be in their final form, essential changes at the proof stage will be considered only exceptionally.

Acknowledgements
If you'd like to thank anyone, place your comments here.

References

[1] R.B. Arellano-Valle and A. Azzalini, A formulation for continuous mixtures of multivariate normal distributions, *Journal of Multivariate Analysis*, 185 (2021), 104780.

[2] R.B. Arellano-Valle, H.W. Gómez and F.A. Quintana. Statistical inference for a general class of asymmetric distributions, *Journal of Statistical Planning and Inference*, 128(2)(2005), 427-443.

[3] A. Azzalini, A class of distributions which includes the normal ones, *Scandinavian journal of statistics*, 12(2)(1985), 171–178.

[4] A. Azzalini and A.D. Valle, The multivariate skew-normal distribution, *Biometrika*, 83(4) (1996), 715–726.

[5] J.C. Bazo-Alvarez, T.P. Morris, J.R. Carpenter and I. Petersen, Current practices in missing data handling for interrupted time series studies performed on individual-level data: A scoping review in health research, *Clinical Epidemiology*, 23(13)(2021), 603–613.

[6] C. Bottomley, J. Scott, G. Anthony and V. Isham, Analysing interrupted time series with a control, *Epidemiologic Methods*, 8(1) (2019), 20180010.

[7] M. Cruz, M. Bender and H. Ombao, A robust interrupted time series model for analyzing complex health care intervention data, *Statistics in Medicine*, 36(29) (2017), 4660–4676.

[8] J. Ewusie, J. Beyene, L. Thabane, S.E. Straus and J.S. Hamid, An improved method for analysis of interrupted time series (ITS) data: accounting for patient heterogeneity using weighted analysis, *International Journal of Biostatistics*, 18(2) (2022), 521–535.

[9] J.E. Ewusie, C. Soobiah, E. Blondal, J. Beyene, L. Thabane and JS. Hamid, Methods, applications and challenges in the analysis of interrupted time series data: A scoping review, *Journal of Multidisciplinary Healthcare*, 13 (2020), 411–423.

[10] C.X. Gao et al., Evaluating the impact of Hazelwood mine fire event on students' educational development with Bayesian interrupted time-series hierarchical meta-regression, *PLoS ONE*, 18(3) (2023), e0281655.

[11] J.F. Gibbons and S. Mylroie, Estimation of impurity profiles in ion-implanted amorphous targets using joined half-Gaussian distributions, *Applied Physics Letters*, 22(11) (1973), 568–569.

[12] H. Jiang, X. Feng, S. Lange, A. Tran, J. Manthey and J. Rehm, Estimating effects of health policy interventions using interrupted time-series analyses: a simulation study, *BMC Medical Research Methodology*, 22(1)(2022), 235.

[13] Korevaar et al., Comparison of statistical methods used to meta-analyse results from interrupted time series studies: an empirical study, *BMC Medical Research Methodology*, 24(2024), 31.

[14] F.D. Leeuwen, P. Lugtig and R. Feskens, The performance of interrupted time series designs with a limited number of time points: Learning losses due to school closures during the COVID-19 pandemic, *PLOS ONE*, 19(8) (2024), 1–23.

[15] W. Liu et al., Simulation-based power and sample size calculation for designing interrupted time series analyses of count outcomes in evaluation of health policy interventions, *Contemporary Clinical Trials Communications*, 17 (2020), 100474.

[16] S. Malladi and Q. Lu, Intervention time series analysis and forecasting of organ donor transplants in the US during the COVID-19 era, *Forecasting*, 5 (2023), 229–255.

[17] J. Nichols, M. Mamdani, T. Gomes, B.R. Shah, C.G. Casey and C.H. Yu, Impact of clinical practice guidelines on blood glucose test

strip prescription rates in Manitoba and Saskatchewan (Canada): An interrupted time-series analysis, *Canadian Journal of Diabetes*, 45(6)(2021), 557–565.

[18] A.L. Schaffer, T.A. Dobbins and S.A. Pearson, Interrupted time series analysis using autoregressive integrated moving average (ARIMA) models: a guide for evaluating large-scale health interventions, *BMC Medical Research Methodology*, 21(1) (2021), 58.

[19] S.L. Turner, et al., Design characteristics and statistical methods used in interrupted time series studies evaluating public health interventions: a review, *Journal of Clinical Epidemiology*, 122 (2020), 1–11.

[20] S.L. Turner, A.B. Forbes, A. Karahalios, M. Taljaard and J.E. McKenzie, Evaluation of statistical methods used in the analysis of interrupted time series studies: a simulation study, *BMC Medical Research Methodology*, 21 (2021), 181.

[21] H. Xiao, O. Augusto and B.H. Wagenaar, Reflection on modern methods: a common error in the segmented regression parameterization of interrupted time-series analyses, *International Journal of Epidemiology*, 50(3) (2021), 1011–1015.

[22] W. Zhang and K. Ning, Spatiotemporal heterogeneities in the causal effects of mobility intervention policies during the COVID-19 outbreak: A spatially interrupted time-series (SITS) analysis, *Annals of the American Association of Geographers*, 113(5) (2023), 111–1134.

Fatemeh Pooyannik
Ph.D. Student
Department of Statistics
Marv.C., Islamic Azad University
Marvdasht, Iran
E-mail: f.pooyannik@gmail.com

Zahra Khodadadi
Assistant Professor of Statistics

Department of Statistics
Marv.C., Islamic Azad University
Marvdasht, Iran
E-mail: zkhodadadi@iau.ac.ir